

INFERRED RESOLUTION THROUGH HERD IMMUNITY OF FIRST COVID-19 WAVE IN MANAUS, BRAZILIAN AMAZON

*Thomas A. A. Prowse, School of Mathematical Sciences, The University of Adelaide, Adelaide, South Australia 5005, Australia

*Tara Purcell, Victorian Infectious Diseases Reference Laboratory Epidemiology Unit at The Peter Doherty Institute for Infection and Immunity, The University of Melbourne and Royal Melbourne Hospital, Melbourne, Victoria 3000, Australia

Djane Clarys Baía-da-Silva, Fundação de Medicina Tropical Dr Heitor Vieira Dourado, Manaus, Brazil

Vanderson Sampaio, Fundação de Vigilância em Saúde; Fundação de Medicina Tropical Dr Heitor Vieira Dourado, Manaus, Brazil

Wuelton Marcelo Monteiro, Universidade do Estado do Amazonas; Fundação de Medicina Tropical Dr Heitor Vieira Dourado, Manaus, Brazil

James Wood, School of Population Health, UNSW Sydney, Australia

Ivo Mueller, Population Health and Immunity Division, Walter + Eliza Hall Institute, Parkville, Victoria, Australia; Department of Medical Biology, FMDHS, Univ. of Melbourne, Parkville; Department of Parasites and Insect Vectors, Institut Pasteur, Paris, France

Jodie McVernon, Victorian Infectious Diseases Reference Laboratory Epidemiology Unit at The Peter Doherty Institute for Infection and Immunity, The University of Melbourne and Royal Melbourne Hospital, Melbourne, Victoria 3000, Australia; Centre for Epidemiology and Biostatistics, Melbourne School of Population and Global Health, The University of Melbourne; Infection and Immunity Theme, Murdoch Childrens Research Institute, Parkville.

#Marcus V. G. Lacerda, Instituto Leônidas & Maria Deane, Fiocruz; Fundação de Medicina Tropical Dr Heitor Vieira Dourado, Manaus, Brazil

#Joshua V. Ross, School of Mathematical Sciences, The University of Adelaide, Adelaide, South Australia 5005, Australia

* equal first authors

equal last authors

NOTE: This preprint reports new research that has not been certified by peer review and should not be used to guide clinical practice.

1 **INTRODUCTORY PARAGRAPH (189 words)**

2 As in many other settings, peak excess mortality preceded the officially reported ‘first wave’
3 peak of the COVID-19 epidemic in Manaus, Brazil, reflecting delayed case recognition and
4 limited initial access to diagnostic testing. To avoid early information bias, we used detailed
5 age and gender stratified death certificate and hospitalisation data to evaluate the epidemic’s
6 trajectory and infer the cause of its decline using a stochastic model. Our results are consistent
7 with heterogenous transmission reducing over time due to the development of herd immunity.
8 Relative to a baseline model that assumed homogenous mixing across Manaus, a model that
9 permitted a small, self-isolated population fraction raised the estimated herd-immunity
10 threshold from 28% to 30% and reduced the final attack rate from 86% to 65%. In the latter
11 scenario, a substantial proportion of vulnerable, older individuals remained susceptible to
12 infection. Given uncertainties regarding the distancing behaviours of population subgroups
13 with different social and economic characteristics, and the duration of sterilising or
14 transmission-modifying immunity in exposed individuals, we conclude that the potential for
15 epidemic outbreaks remains, but that future waves of infection are likely to be much less
16 pronounced than that already experienced.

17 **LETTER TEXT (1,495 words)**

18 ***Background/Rationale (420 words)***

19 Globally, marked differences have been observed in morbidity and mortality due to SARS-
20 CoV-2 infection. This variability mostly reflects the extent and timeliness of spontaneous and
21 imposed changes in social mixing and the sensitivity of surveillance systems to detect cases
22 and deaths¹. Many countries that successfully constrained the initial epidemic through
23 distancing measures are now experiencing second waves in still-susceptible populations².

24 Estimates of R_0 for SARS-CoV-2 in the range 2 to 6^{3,4} suggest that population immunity of
25 approximately 50-80% is required to achieve herd protection. However, heterogeneous
26 behaviour, infectivity and immunity within subpopulations could plausibly decrease this
27 threshold to 10-20%⁵. Controversy remains regarding the extent of population exposure
28 required to achieve such constraint⁶.

29 Comparison of population attack rates to inform this question is made challenging by
30 imperfect case ascertainment, compounded by limited diagnostics and overwhelmed health
31 systems, particularly in high incidence settings. Assessment of epidemic activity therefore
32 requires the use of less biased metrics than confirmed case reports. Excess mortality is an
33 objective measure which, with cause-of-death certification, can be used as an indicator of
34 direct and indirect COVID-19 associated mortality⁷. With hospitalisations data, it can inform
35 retrospective estimation of cumulative cases and deaths⁸.

36 Brazil experienced a severe first wave of COVID-19 disease, with mass mortality reported in
37 many states, mainly in the north where seasonality of respiratory infections contributed to
38 higher vulnerability. A socialized health system provided free and global access to tertiary care
39 hospitals, but inequalities might explain different mortality rates in the population⁹. In Manaus,
40 the highly urbanised capital of Amazonas state, the first case of COVID-19 was reported on 13
41 March 2020¹⁰. By 11 August 2020, 37,597 cases and 2,051 deaths were reported¹¹.

42 However, burial and death records indicate far higher mortality than official reports, suggesting
43 late recognition of importation and underreporting. Previous studies have assumed that the first
44 wave in Manaus was significantly mitigated by non-pharmaceutical interventions (NPIs)¹².
45 While these restrictions may have partly constrained early transmission, local reports indicate
46 that implementation was highly variable¹³. Moreover, a possible role for immunity is suggested
47 by the observation of declining cases and deaths over a period in which restrictions were
48 officially eased.

49 We use death certificate and hospitalisation records to parameterise an epidemiological model
50 of the COVID-19 epidemic in Manaus. The model allows inference of age- and gender-
51 stratified infection-fatality ratios to explore evidence for development of herd immunity as a
52 driver of local epidemic resolution, with implications for the ongoing risk posed by SARS-
53 CoV-2 to this population.

54 ***Main results (388 words)***

55 We calculated 3,457 excess deaths in Manaus, Brazil, between 19 March and 24 June 2020
56 (Supplementary Table 1) representing 0.16% of the city's population. Males 30 years and over
57 experienced greater excess mortality than females; individuals aged 75 years or more
58 accounted for 39% of the excess (Figure 1a). During this period, 7% of the 75+ male population

59 in Manaus died (Figure 1b). COVID-19 deaths were first reported from 26 March and increased
60 weekly thereafter in keeping with improved access to diagnostics and/or increasing prevalence
61 (Figure 2), comprising 53% of the total excess. Other reported causes of death included
62 respiratory diseases, unattended and unknown causes of mortality, cardiovascular, endocrine
63 and cancer-related mortality, the majority of which were compatible¹⁴ with a clinical diagnosis
64 of COVID-19 or are known comorbidities associated with severe outcomes (Figure 2).

65 Stochastic transmission models captured the observed peak in excess deaths in late April,
66 including age and gender variation (Figure 3, Supplementary Figures S1, S3). The models also
67 captured synchronous peaks in hospitalisations (Figure 3, Supplementary Figures S2, S4),
68 although model fit to these data was poorer, potentially reflecting delayed recognition of
69 COVID-19 cases and/or capacity exceedance during the epidemic peak.

70 Despite their different assumptions about the proportion of the Manaus population at risk, the
71 two model scenarios yielded equivalent fits to the data (Figure 3A, B). The baseline model
72 estimated heterogenous transmission ($k=0.065$ [0.047, 0.093], mean [95 % credible intervals]),
73 a mean time-to-death of 13 days (Supplementary Figures S5), and inferred a population-wide
74 attack rate of 85.7 [84.6, 86.7]% by 20 July. Attack rates were lowest in younger age classes
75 (Figure 3A(i)), reflecting lower susceptibility assumed for people under 15 years.

76 Infection fatality rate (IFR) estimates for the baseline model ranged from almost zero for both
77 genders aged 30-35 years, to 3.0 [2.8, 3.3]% and 7.4 [6.8, 8.0]% for females and males over 75
78 years, respectively (Figure 4). At a population level, reduced mobility resulted in variable R_t ,
79 while estimates of R_{eff} fell below 1 after 10 April (Supplementary Figure S6), when the
80 estimated attack rate was 52.6 [51.1, 54.1]%.

81 Outcomes were similar for the second model which estimated 24.5 [23.0, 25.1]% of the Manaus
82 population was effectively removed from the susceptible pool. Relative to the baseline model,
83 this second model raised the calculated herd-immunity threshold from 28% to 30% and reduced
84 the final attack rate to 65.0 [63.7, 65.6]%.

85 ***Implications (687 words)***

86 Early time-series modelling of the COVID-19 epidemic in Brazilian states up to 6 May 2020
87 used an unstructured model informed by state-level mobility indicators and reported deaths¹².
88 The model inferred population attack rates ranging from 0.13% to 10.6%, for Minas Gerais
89 and Amazonas, respectively, and predicted ongoing epidemic growth throughout May. Other
90 modelled R_0 estimates based on reported COVID-19 cases from Amazonas state have similarly
91 anticipated continued growth in cases through the month of June¹³. These models could neither
92 explain nor accurately forecast observations of epidemic decline in Manaus.

93 Our analysis of excess deaths and hospitalisations in Manaus identifies rapid epidemic growth
94 from late March, peaking in late April, with a return to baseline mortality in early June. These
95 age- and gender-stratified models inferred heterogeneous transmission consistent with previous
96 studies of SARS-CoV-1¹⁵ and SARS-CoV-2¹⁶, and a herd-immunity threshold of around 30%.
97 However, we estimated that this threshold was substantially overshot in Manaus, with resulting
98 attack rates inferred to be 86% and 65% for models that assumed the risk of infection applied
99 to 100% or *c.* 75% of the population, respectively.

100 Although both models estimated declining SARS-CoV-2 transmission over time due to herd
101 immunity, their implications for the possibility of subsequent waves are qualitatively different.
102 Although there are currently no data to support the assertion that some fraction of the Manaus
103 population self-isolated, we consider the second model is likely more realistic because: (1) the
104 estimated infection-fatality ratios are higher than reported from high-income countries¹⁷ which
105 we anticipate to be plausible; and (2) a population attack rate of 65% is more consistent with
106 recent estimates based on a Manaus blood bank serosurvey¹⁸ which reported the largest
107 increase in seropositivity over the month of April.

108 We focus on Manaus as the epicentre of the COVID-19 epidemic in Amazonas, avoiding
109 conflation of case numbers in this dense city of more than 2 million people with slower
110 growing rural outbreaks across the state⁶. Given known information bias associated with
111 limited early testing capacity, we used excess deaths and hospitalisations as the most
112 objective indicators of epidemic activity presently available. Detailed cause-of-death data
113 support the hypothesis that the majority of excess mortality over this time was COVID-19
114 related.

115 An important caveat is that estimated attack rates accumulate all infections and are agnostic to
116 the presence or degree of symptoms. Severity of the clinical course of COVID-19 is associated
117 with magnitude and persistence of the host immune response¹⁹. In consequence, our estimates
118 of ‘exposure’ cannot be directly related to predicted antibody seroprevalence at the end of the
119 first wave²⁰. It is reasonably anticipated that population immunity will wane over time,
120 requiring robust memory responses²¹ to prevent reinfection or modify the clinical course²².

121 Our findings support emerging evidence that population heterogeneity of SARS-CoV-2
122 transmission, attributable to a range of biological and sociological factors, reduces the herd
123 immunity threshold^{16,23,24}. Reduction of superspreading events through constraints on mixing
124 group sizes is concordant with genomic studies showing successive extinction of imported
125 strains under the influence of social and mobility restrictions²⁵.

126 While future infection clusters and outbreaks remain possible in Manaus due to unexposed
127 subgroups, population-level immunity will likely constrain widespread transmission unless
128 immunity wanes. As in other settings, underlying vulnerability of older age groups may be
129 further exacerbated over time by reduced health seeking behaviours of individuals with pre-
130 existing and new medical conditions²⁶. Social measures should be informed by understanding
131 of key enablers of superspreading and amplification, awareness of at-risk populations and
132 tailored to context depending on population experience of the first wave.

133 Excess mortality data are not sufficiently timely to support real-time decision making, but in
134 areas with limited testing may be a more reliable indicator of past epidemic activity than
135 confirmed cases. To accurately support response to and assess the impact of the COVID-19
136 and other public health emergencies, improved access to diagnostics, and strengthening of
137 reporting systems are needed in low- and middle-income settings. Cross-sectional and
138 longitudinal seroprevalence studies are essential to understand markers and maintenance of
139 immunity to inform prediction of long-term epidemiologic trends and bridging to likely vaccine
140 impacts^{18,27}.

141 *Acknowledgements*

142 TAAP is supported by the NHMRC Centre for Research Excellence in Policy Relevant
143 Infectious Disease Simulation and Mathematical Modelling. JM is supported by an NHMRC

144 Principal Research Fellowship GNT1117140. IM is supported by an NHMRC Principal
145 Research Fellowship GNT1155075.

146 **METHODS (ONLINE ONLY)**

147 *Excess mortality and reported causes*

148 Death certificate data from January 2015 to June 2020 were sourced from the Brazilian
149 Ministry of Health Mortality Information System (SIM). Information on age, gender, and
150 cause and date-of-death was recorded. Cause of death was reported using the World Health
151 Organization's (WHO) International Classification of Diseases 10th revision (ICD-10). The
152 2010 population census and the 2019 municipal population estimates were accessed from the
153 Brazilian Institute of Geography and Statistics (IBGE). This project was approved by the
154 *Fundação de Medicina Tropical Dr Heitor Vieira Dourado* Ethics Review Board (Approval
155 4.033.218).

156 Background mortality was calculated by averaging the number of deaths observed per week,
157 commencing on January 1 each year, for the previous 5 years (2015-2019). Background
158 mortality was further stratified by gender and into 5-year age bands, culminating at 75+. For
159 each subgroup, we subtracted this five-year average from deaths observed for the period
160 between March 19 and June 24 of 2020 to determine excess deaths. This period was selected
161 as excess mortality was first observed in the week beginning on March 19 and the data returned
162 to baseline background mortality in the week beginning on June 25.

163 The age and gender structure reported in the 2010 population census was used to estimate the
164 2019 population size for each age and gender class. Population estimates were aggregated into
165 5-year age bands. The 5-year population estimates for 2019 were used to determine excess
166 mortality, as a proportion of the population.

167 The ICD-10 codes assigned to each death certificate were aggregated into 7 categories: diseases
168 of the respiratory system (J00-J99), circulatory system (I00-I99), endocrine system (E00-E99),
169 unattended (R98) and unknown cause of death (R99), coronavirus infection (B34.2) and all
170 remaining codes were categorised as 'other'. All analyses were performed using R software.

171 *Hospitalisation data*

172 Hospitalisation data for patients admitted to all hospitals (private and public) in Manaus from
173 January 2020 to July 2020 was accessed from the Influenza Surveillance Information System
174 (SIVEP-Gripe). Data entry in this system is compulsory by law. A deidentified line list

175 included patient demographics, comorbidities, clinical symptoms, investigations, clinical
176 management and outcome data.

177 Daily admissions to both hospital and intensive care units (ICU) were aggregated each week
178 in 2020 and stratified into 3 age bands (0-29, 30-64 and 65+). For each week, the proportion
179 of hospital and ICU admissions within each age group was determined. Between April and
180 July, the proportional distribution of hospital and ICU admissions across the three categories
181 remained fairly stable, with no evidence of rationing of service access on the basis of age.

182 *Epidemiological model*

183 We developed a stochastic, discrete-time, susceptible-infected-recovered epidemiological
184 model for Manaus which we calibrated using daily time-series data from the death-certificate
185 and hospitalisation records. The model assumed an initial population size equal to that of
186 Manaus in 2019 (2,182,761), which was split into $N=36$ age/gender groups based on
187 proportions reported in the 2010 census (i.e., 5-year age classes up to an age of 75 years, and
188 then a pooled age class for all individuals aged 75 years and over). To allow inference on the
189 background mortality rate in each age/gender group, the model was initiated on January 1,
190 2020, approximately two months prior to the introduction of COVID-19. The model was
191 terminated after $n=202$ days on July 20, 2020, to ensure complete reporting of both death
192 certificates and hospitalisations over the modelled period. The model detailed below was fitted
193 within a Bayesian framework using *JAGS* (v. 4.3.0) software²⁸ and a mixture of informative
194 and uninformative priors (for full details of the model code, including details of all prior
195 distributions, see Supplementary Appendix S1).

196 ***COVID-19 introduction and virus transmission.*** We initialised the model by allowing
197 importation of COVID-19 cases into Manaus over the week beginning March 5, 2020 (one
198 week before the first reported case), and inferred an importation model such that the number
199 of introduced cases into each group in each day of this first week arose from a Poisson process
200 with a common mean inferred from the data. To model community transmission, we inferred
201 a reproduction number on day t that was modified by an index of human mobility

$$202 \quad R_t = e^{(\log(R_0) + aX_t)}$$

203 where R_0 is the basic reproduction number, X_t is the mobility covariate and a is the inferred
204 coefficient. We derived the time-series X_t by first averaging daily data for five separate indices
205 of community mobility (available as the mobility change relative to baseline for
206 retail/recreation, grocery/pharmacy, parks, transit stations and workplaces, accessed from
207 www.google.com/covid19/mobility), and then smoothed the series with a 7-day moving-
208 average smoother. We then assumed the effective reproduction number $R_{eff(i,j,t)}$ in group i due
209 to mixing with group j on day t is

$$210 \quad R_{eff(i,j,t)} = R_t Q_i M_{i,j} S_{i,t}$$

211 where Q_i is the susceptibility of group i to infection, $M_{i,j}$ is the rate of mixing between the two
212 groups, and $S_{i,t}$ is the time-varying proportion of susceptible (previously uninfected)
213 individuals remaining in the focal group. Based on previous studies^{29,30}, we used prior means
214 for the susceptibilities of 0-15, 15-60, and 60+ year old age classes of 0.5, 1.0, and 1.3,
215 respectively.

216 Mixing between groups was governed by an age-structured mixing matrix reported previously
217 for Brazil³¹, which we corrected to be symmetrical (by averaging the upper and lower
218 triangles), scaled to a mean of $1/N$, and applied equally to both genders. The expected number
219 of new cases in each group each day was then calculated as

$$220 \quad C_{i,t} = \sum_{j=1}^N R_{eff(i,j,t)} (c_{j,1:(t-1)} \cdot g_{(t-1):1})$$

221 where $c_{j,1:(t-1)}$ is the case-history vector for group j and $g_{(t-1):1}$ is the portion of the generation
222 interval distribution relevant to those cases. We used the same generation interval distribution
223 as Mellan et al.¹² which concentrated >99% of an individual's infectivity within the first 3
224 weeks of infection (median generation interval=5 days).

225 To account for heterogeneity in transmission, we assumed the offspring distribution in group i
226 due to mixing with infectious individuals from group j on day t was governed by a negative
227 binomial distribution with mean equal to $C_{i,t}$ and variance equal to $C_{i,t}(1 + C_{i,t}/\Phi_{i,t})$, where

$$228 \quad \Phi_{i,t} = kC_{i,t}/R_t$$

229 and k is the overdispersion parameter, such that smaller values of k represent greater
230 transmission heterogeneity (i.e., the more transmission is due to a small number of people,
231 including by so-called “superspreaders”). Given no previous study has documented strong
232 evidence of different susceptibility between genders, we first generated the expected number
233 of new cases in each age class (regardless of gender), and then assumed gender-specific cases
234 arose from a binomial distribution with probability equal to the proportion of the total
235 susceptible individuals for that age class attributable to each gender.

236 **Background and COVID-induced mortality.** We developed a model for the expected number
237 of deaths per day which was comprised of three components. First, we modelled the
238 background (pre-COVID-19) death rate d_i estimated separately for each group. Second,
239 available data on the time from symptom onset to death for confirmed COVID-19 cases (from
240 the Manaus hospitalisation records) were used to infer a 4-parameter (y_0, u_{\min}, u_0, b) mortality
241 distribution (m) as a function of the time x since symptom onset ($x \in \{-5, \dots, N-5\}$) of the form

$$242 \quad m_{x+a} = \frac{y_0 e^{u_{\min}(x+a)} + ((u_0 - u_{\min})/b)(1 - e^{-b(x+a)})}{\sum_{j=1}^N m_j}$$

243 where a is the average time from infection to symptoms, which was fixed at 5 days^{3,32,33}.
244 Finally, we modelled the infection-fatality ratio in each group i (IFR_i) as a log-linear function
245 of age and gender, with prior distributions on this components’ parameters based on a recent
246 meta-analysis of COVID-19-induced mortality³⁴. Together, these components yielded the
247 following model for the expected number of deaths

$$248 \quad D_{i,t} = d_i + IFR_i \sum_{j=1}^N (c_{j,1:(t-1)} \cdot m_{(t-1):1})$$

249 and the observed number of deaths each day was assumed to arise from a Poisson distribution
250 with mean equal to $D_{i,t}$.

251 **Hospitalisations due to COVID-19.** Hospitalisations were modelled in a similar way to
252 COVID-induced deaths, in that available data on the time from symptom onset to
253 hospitalisation were used to infer a 4-parameter hospitalisation distribution (h) of the same
254 functional form as that used for the mortality distribution above. We modelled the infection-

255 hospitalisation ratio in each group i (IHR_i) as a logistic function of age and gender. Daily
256 hospitalisations were assumed to arise from a Poisson distribution with mean equal to

257
$$H_{i,t} = IHR_i \sum_{j=1}^N (c_{j,1:(t-1)} \cdot h_{(t-1):1}) .$$

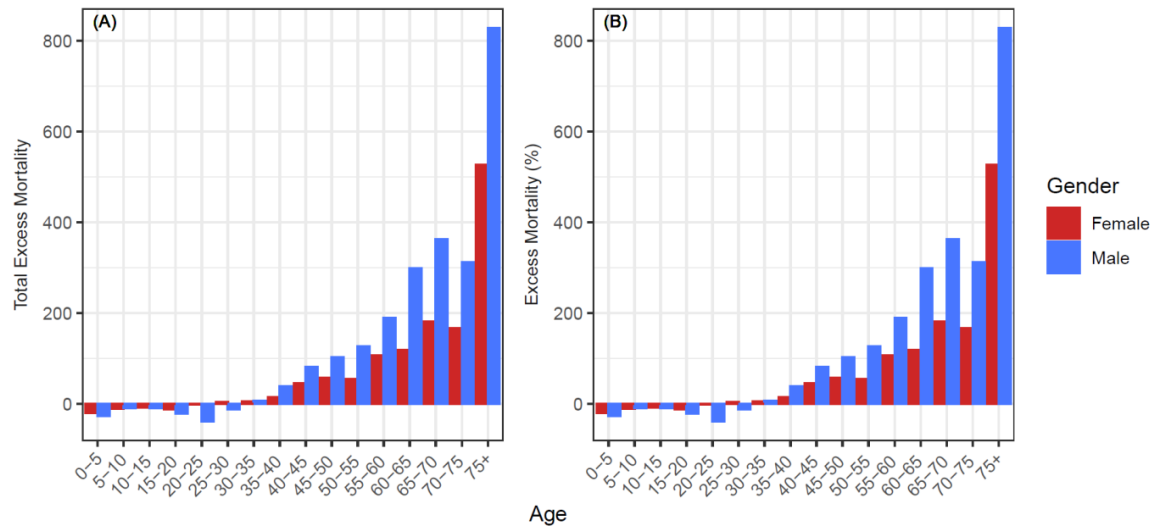
258 **Model scenarios.** Given no data were available on whether some portion of the Manaus
259 population has been self-isolating since March 2020, we initially fitted a ‘baseline’ model to
260 death-certificate and hospitalisation data which assumed homogeneous age-structured mixing
261 across the entire Manaus population. We compared these model outcomes to those from a
262 second model that permitted a self-quarantined proportion of the population which could not
263 be exposed to the SARS-CoV-2 virus. Communication with local experts including authors on
264 this paper suggested that more wealthy residents of Manaus had been able to greatly reduce
265 social interactions during the first epidemic wave and avoid exposure to the virus. We reviewed
266 detailed socio-demographic data on Manaus³⁵, but were not able to source quantitative
267 estimates of the relevant population fraction. However, we considered that this would not
268 exceed the upper 2 income quintiles (40%) of the population but was likely to be greater than
269 the wealthiest 10%, and accordingly, chose a non-informative uniform (0.1,0.4) prior on this
270 population fraction.
271

272 REFERENCES

- 273 1. Dye, C., Cheng, R., Dagpunar, J. & Williams, B. The scale and dynamics of COVID-
274 19 epidemics across Europe.
275 (<https://www.medrxiv.org/content/10.1101/2020.06.26.20131144v2>, 2020).
- 276 2. Klein, A. Australia looks to be finally beating its second wave of coronavirus. in *New*
277 *Scientist* ([https://www.newscientist.com/article/2252690-australia-looks-to-be-finally-](https://www.newscientist.com/article/2252690-australia-looks-to-be-finally-beating-its-second-wave-of-coronavirus)
278 [beating-its-second-wave-of-coronavirus](https://www.newscientist.com/article/2252690-australia-looks-to-be-finally-beating-its-second-wave-of-coronavirus), 2020).
- 279 3. Li, Q., *et al.* Early Transmission Dynamics in Wuhan, China, of Novel Coronavirus–
280 Infected Pneumonia. **382**, 1199-1207 (2020).
- 281 4. Sanche, S., *et al.* High Contagiousness and Rapid Spread of Severe Acute Respiratory
282 Syndrome Coronavirus 2. *Emerging Infectious Disease journal* **26**, 1470 (2020).
- 283 5. Aguas, R., *et al.* Herd immunity thresholds for SARS-CoV-2 estimated from
284 unfolding epidemics. 2020.2007.2023.20160762 (2020).
- 285 6. Ferrante, L., *et al.* Brazil’s policies condemn Amazonia to a second wave of COVID-
286 19. *Nature Medicine* (2020).
- 287 7. Felix-Cardoso, J., Vasconcelos, H., Rodrigues, P. & Cruz-Correia, R. Excess
288 mortality during COVID-19 in five European countries and a critique of mortality
289 analysis data. 2020.2004.2028.20083147 (2020).
- 290 8. Thompson, R.N., *et al.* Key questions for modelling COVID-19 exit strategies. *Proc*
291 *Biol Sci* **287**, 20201405 (2020).
- 292 9. Croda, J., *et al.* COVID-19 in Brazil: advantages of a socialized unified health system
293 and preparation to contain cases %J *Revista da Sociedade Brasileira de Medicina*
294 *Tropical*. **53**(2020).
- 295 10. Amazonas Health Surveillance Foundation FVS. Amazonas confirms 1st case of
296 Covid-19 and authorities guarantee that the assistance network is prepared for
297 assistance. (2020).
- 298 11. Amazonas Health Surveillance Foundation FVS. COVID-19 Monitoring Panel.
299 Manaus, Brazil. (2020).
- 300 12. Mellan, T.A., Hoeltgebaum, H.H. & Mishra, S. Estimating COVID-19 cases and
301 reproduction number in Brazil. (Imperial College London, 2020).
- 302 13. de Souza, W.M., *et al.* Epidemiological and clinical characteristics of the COVID-19
303 epidemic in Brazil. *Nat Hum Behav* **4**, 856-865 (2020).
- 304 14. Excess deaths associated with COVID-19. Provisional death counts for coronavirus
305 disease (COVID-19). National Center for Health Statistics, Centers for Disease
306 Control and Prevention.
- 307 15. Lloyd-Smith, J.O., Schreiber, S.J., Kopp, P.E. & Getz, W.M. Superspreading and the
308 effect of individual variation on disease emergence. *Nature* **438**, 355-359 (2005).
- 309 16. Endo, A., null, n., Abbott, S., Kucharski, A. & Funk, S. Estimating the overdispersion
310 in COVID-19 transmission using outbreak sizes outside China [version 3; peer
311 review: 2 approved]. **5**(2020).
- 312 17. Levin, A., Meyerowitz-Katz, G., Owusu-Boaitey, N., Cochran, K. & Walsh, S.
313 Assessing the age specificity of infection fatality rates for COVID-19: systematic
314 review, meta-analysis, and public policy implications.
315 (<https://www.medrxiv.org/content/10.1101/2020.07.23.20160895v4.full.pdf>, 2020).
- 316 18. Buss, L., *et al.* COVID-19 herd immunity in the Brazilian Amazon.
317 (<https://www.medrxiv.org/content/10.1101/2020.09.16.20194787v1>, 2020).
- 318 19. Long, Q.X., *et al.* Clinical and immunological assessment of asymptomatic SARS-
319 CoV-2 infections. *Nat Med* **26**, 1200-1204 (2020).

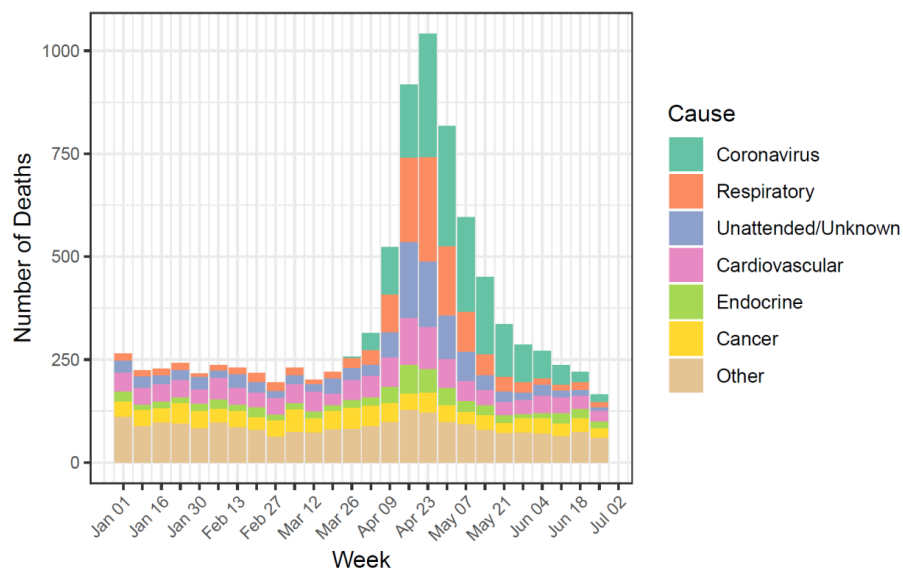
- 320 20. Hallal, P., *et al.* Remarkable variability in SARS-CoV-2 antibodies across Brazilian
321 regions: nationwide serological survey in 27 states.
322 (<https://www.medrxiv.org/content/10.1101/2020.05.30.20117531v1>, 2020).
- 323 21. Rodda, L., *et al.* Functional SARS-CoV-2 specific immune memory persists after
324 mild COVID-19.
325 (<https://www.medrxiv.org/content/10.1101/2020.08.11.20171843v2>, 2020).
- 326 22. Ledford, H. COVID-19 reinfection: three questions scientists are asking. *Nature* **585**,
327 168-169 (2020).
- 328 23. Britton, T., Ball, F. & Trapman, P. A mathematical model reveals the influence of
329 population heterogeneity on herd immunity to SARS-CoV-2. **369**, 846-849 (2020).
- 330 24. Wang, Y. & Teunis, P. Strongly Heterogeneous Transmission of COVID-19 in
331 Mainland China: Local and Regional Variation. **7**(2020).
- 332 25. Pybus, O.G., *et al.* Preliminary analysis of SARS-CoV-2 importation and
333 establishment of UK transmission lineages. ([https://virological.org/t/preliminary-
334 analysis-of-sars-cov-2-importation-establishment-of-uk-transmission-lineages/507](https://virological.org/t/preliminary-analysis-of-sars-cov-2-importation-establishment-of-uk-transmission-lineages/507),
335 2020).
- 336 26. Kluge, H.H.P., *et al.* Prevention and control of non-communicable diseases in the
337 COVID-19 response. *Lancet* **395**, 1678-1680 (2020).
- 338 27. Koopmans, M. & Haagmans, B. Assessing the extent of SARS-CoV-2 circulation
339 through serological studies. *Nat Med* **26**, 1171-1172 (2020).
- 340 28. Plummer, M. JAGS: A Program for Analysis of Bayesian Graphical Models using
341 Gibbs Sampling. *3rd International Workshop on Distributed Statistical Computing*
342 (*DSC 2003*); Vienna, Austria **124**(2003).
- 343 29. Zhang, J., *et al.* Changes in contact patterns shape the dynamics of the COVID-19
344 outbreak in China. **368**, 1481-1486 (2020).
- 345 30. Davies, N.G., *et al.* Age-dependent effects in the transmission and control of COVID-
346 19 epidemics. *Nature Medicine* (2020).
- 347 31. Prem, K., Cook, A.R. & Jit, M. Projecting social contact matrices in 152 countries
348 using contact surveys and demographic data. *PLOS Comput. Biol.* **13**, e1005697
349 (2017).
- 350 32. Lauer, S.A., *et al.* The Incubation Period of Coronavirus Disease 2019 (COVID-19)
351 From Publicly Reported Confirmed Cases: Estimation and Application. *Annals of*
352 *Internal Medicine* **172**, 577-582 (2020).
- 353 33. He, X., *et al.* Temporal dynamics in viral shedding and transmissibility of COVID-19.
354 *Nature Medicine* **26**, 672-675 (2020).
- 355 34. Levin, A.T., Meyerowitz-Katz, G., Owusu-Boaitey, N., Cochran, K.B. & Walsh, S.P.
356 Assessing the age specificity of infection fatality rates for COVID-19: systematic
357 review, meta-analysis, and public policy implications. 2020.2007.2023.20160895
358 (2020).
- 359 35. United Nations Development Programme. Atlas of human development in Brazil
360 (http://www.atlasbrasil.org.br/2013/en/perfil_m/manaus_am/, accessed 16/09/2020).
- 361

362



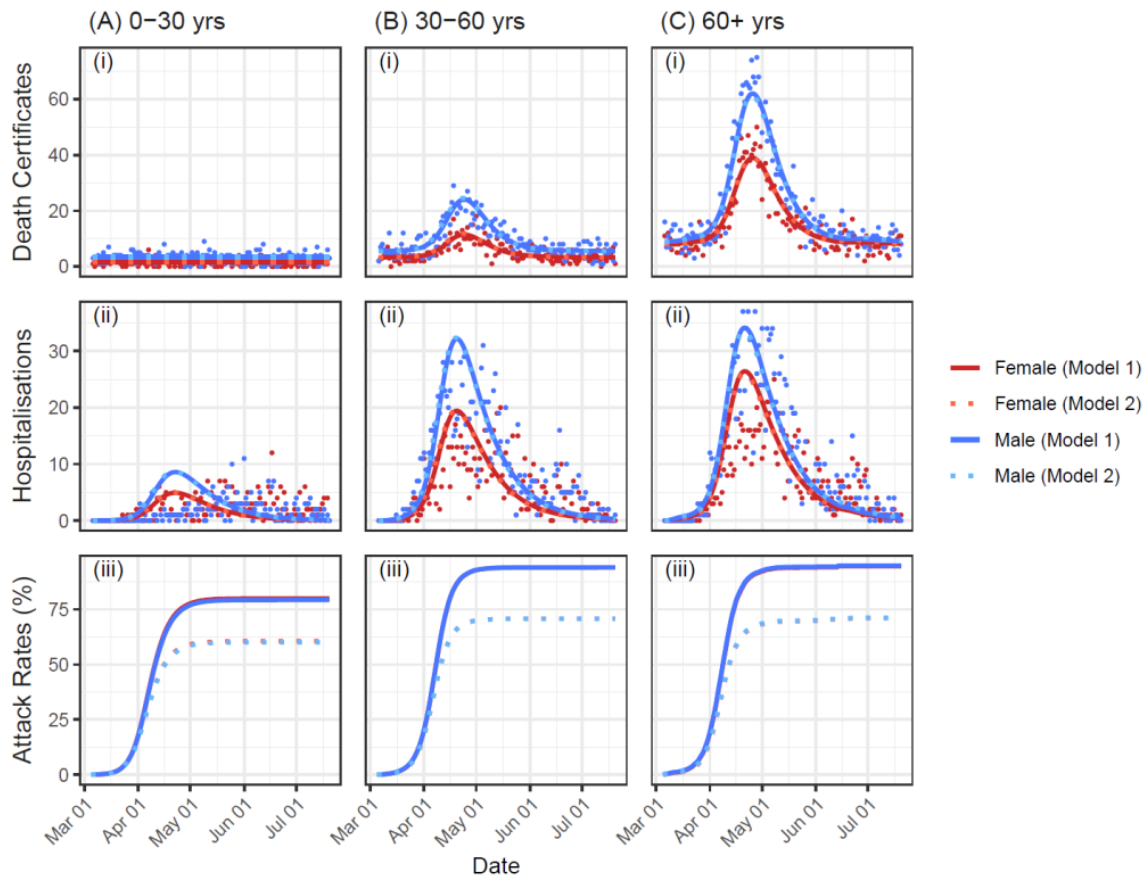
363

364 **Figure 1.** (a) Total excess mortality by age and gender for the period between March 19 and
365 June 24 of 2020. Excess mortality is the 2020 weekly observed mortality less the expected
366 mortality summed for the period between March 19 and June 24 of 2020 for each subgroup.
367 (b) Excess mortality for the period between March 19 and June 24 of 2020 divided by the
368 estimated 2019 subgroup populations to obtain population proportions.



369

370 **Figure 2.** Observed weekly mortality for the period between January 01 and July 22 of 2020
371 aggregated by major ICD-10 categories of attributed causes of death.



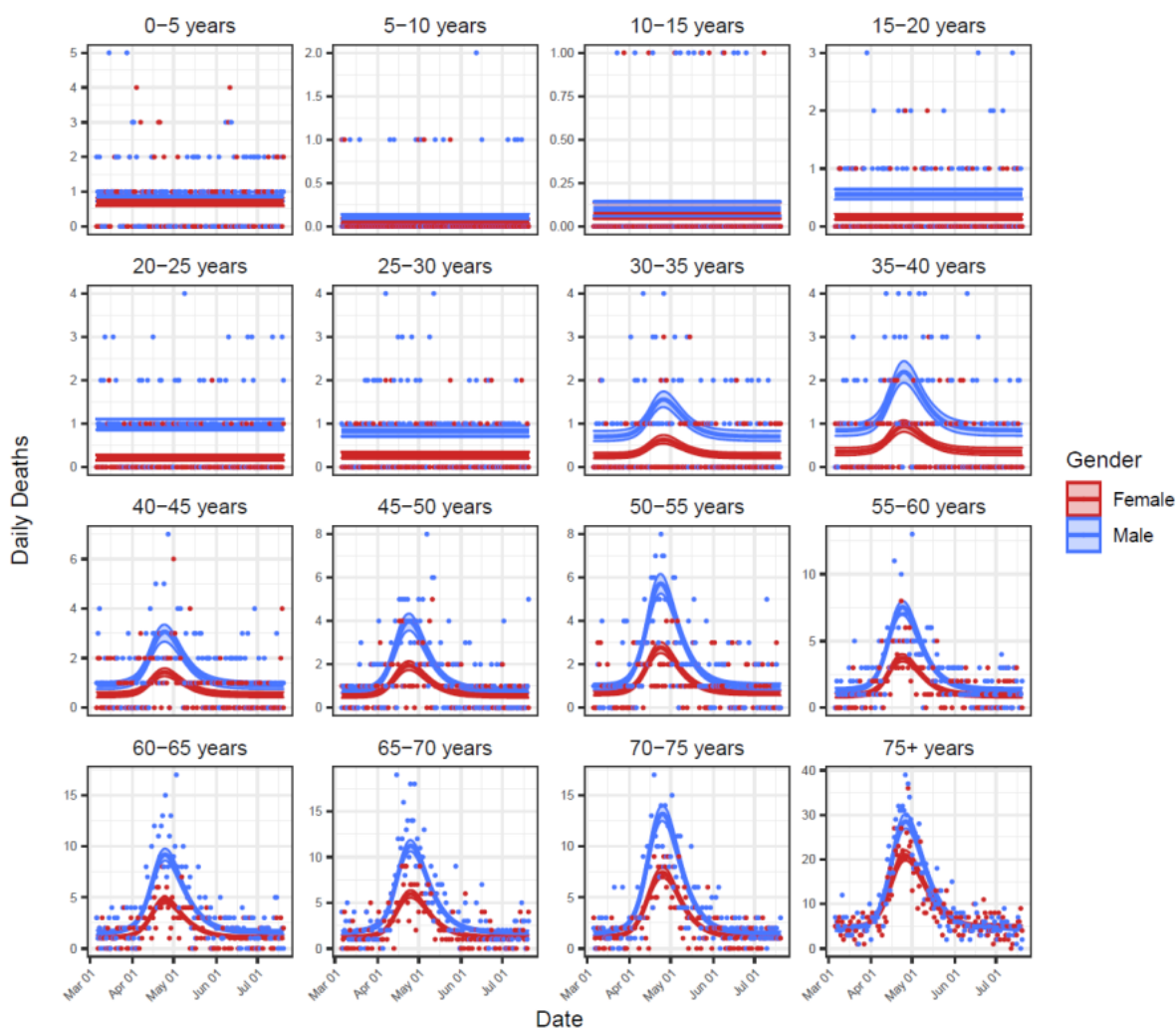
372

373 **Figure 3.** Integrated model fits by gender and model, pooled at the level of three aggregated
374 age classes: (A) 0-30 years; (B) 30-60 years; and (C) 60+ years. For each age class, panels (i)
375 and (ii) show the fit of the model (lines) to the reported number of deaths and hospitalisations
376 per day (points), while panel (iii) shows inferred attack rates. Note that lines showing the
377 model fits overlap in panels (i) and (ii), and attack rates for males and females overlap in
378 panel (iii).

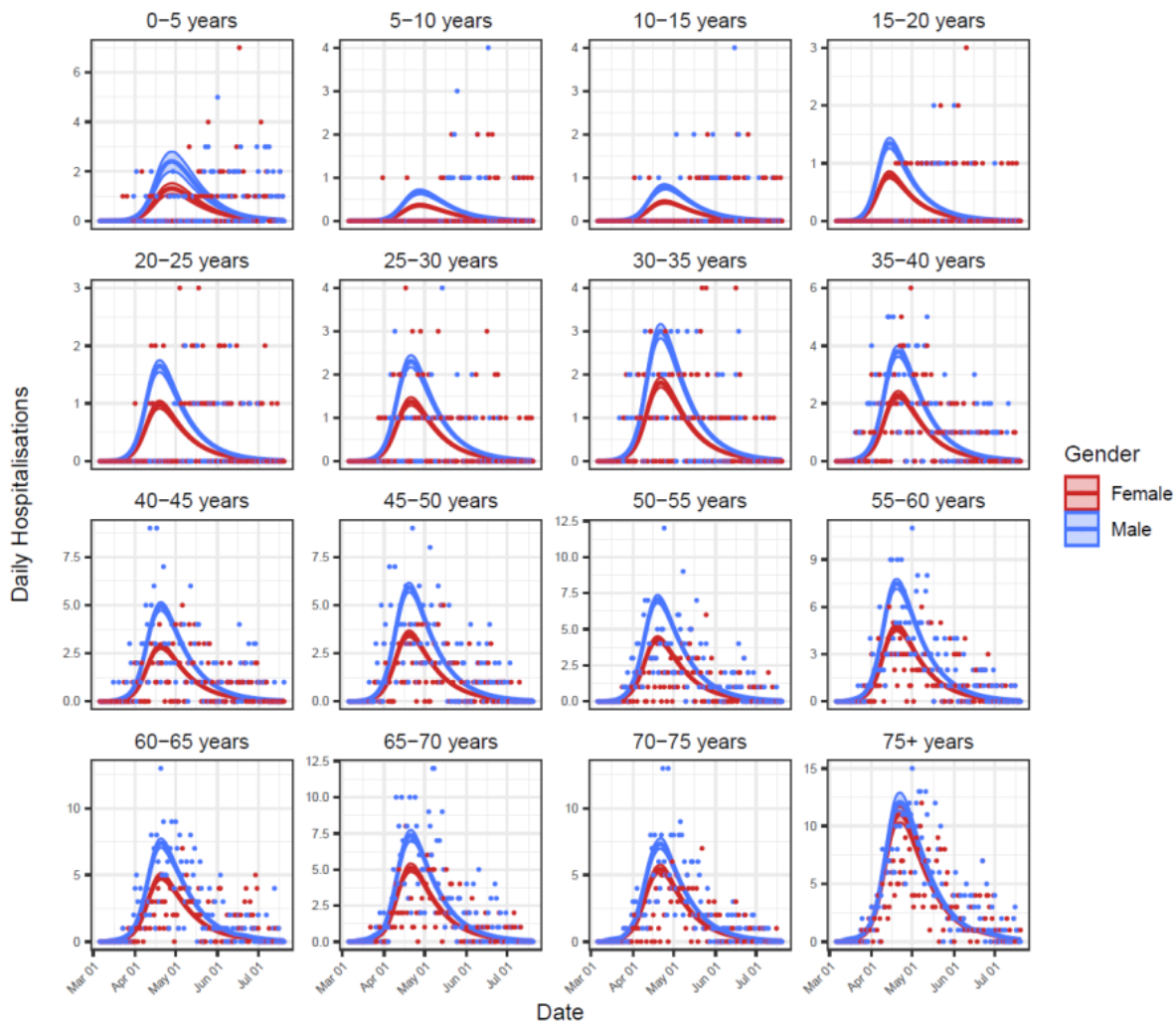


379

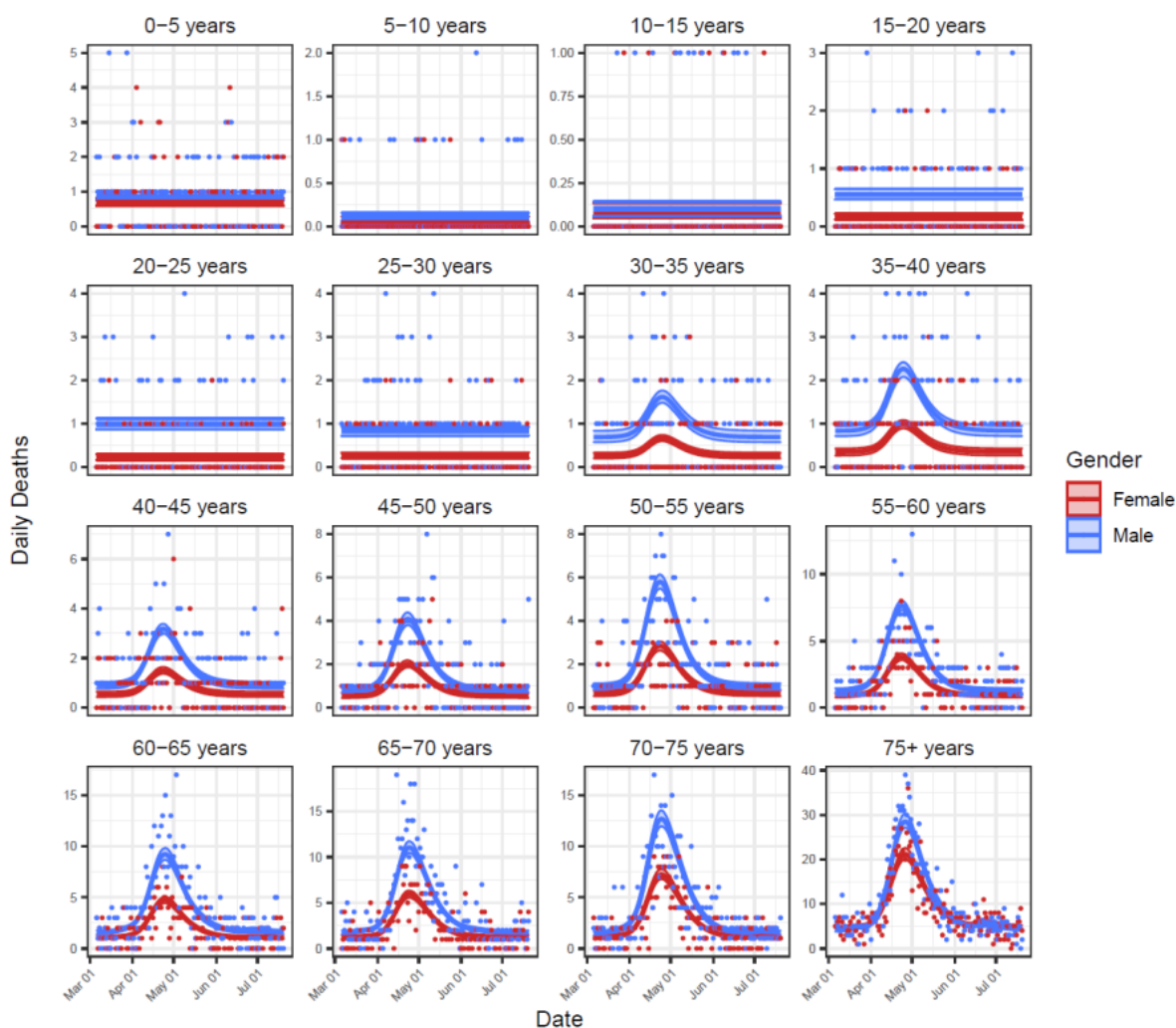
380 **Figure 4.** Model-based estimates (mean \pm 95 % credible intervals) of age- and gender-
381 structured (A) infection-fatality ratios (IFRs) and (B) infection-hospitalisation ratios (IHRs).
382 Note that in panel (A), IFRs were fixed at zero for all age classes below 30 years.



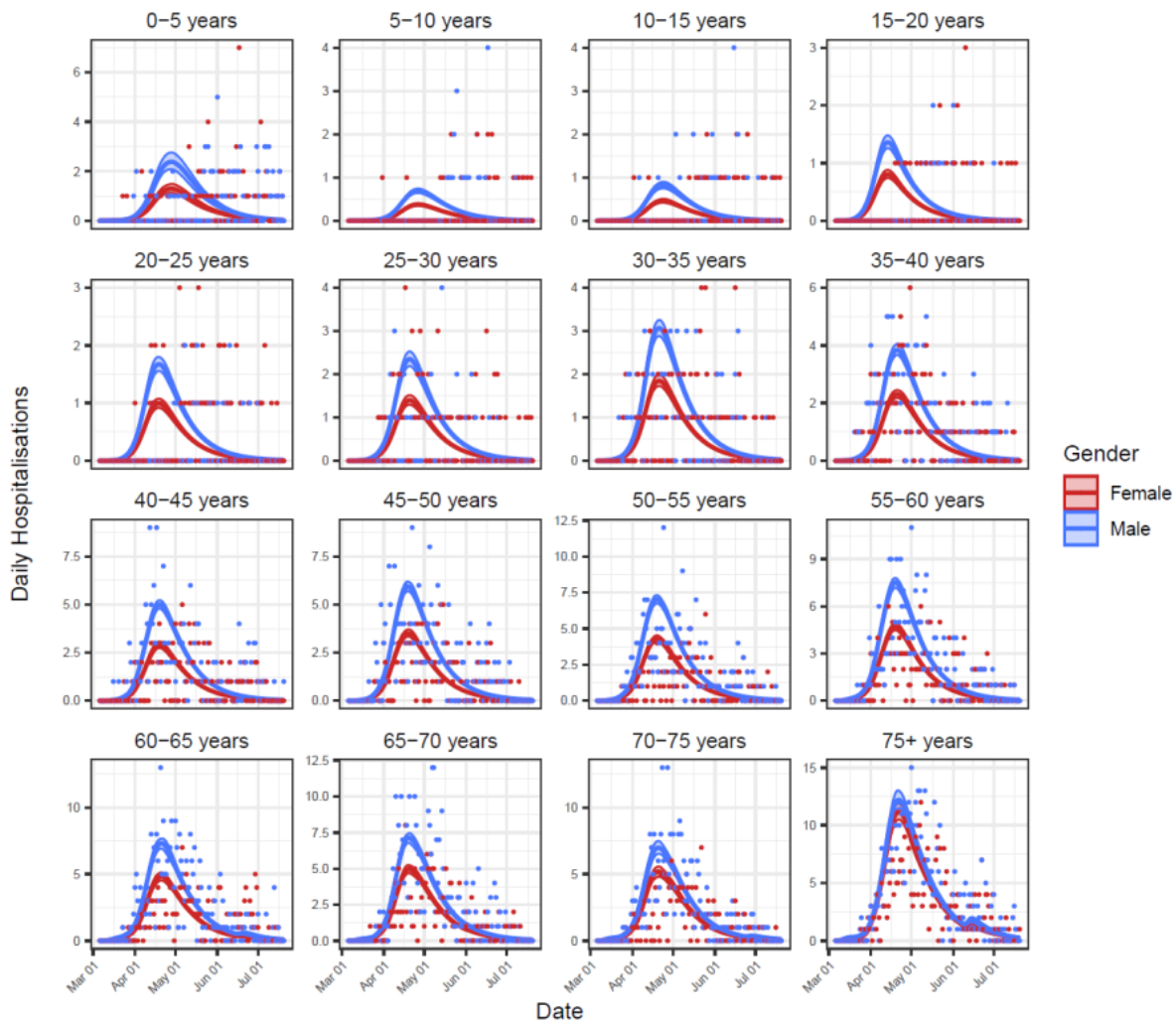
383
384 **Figure S1.** Baseline model fits to daily deaths data for all 32 age and gender classes. Shown
385 are the model-inferred expected death rate from all causes (lines) \pm 95% credible intervals
386 (ribbons), and the mortality data used for model fitting (points).



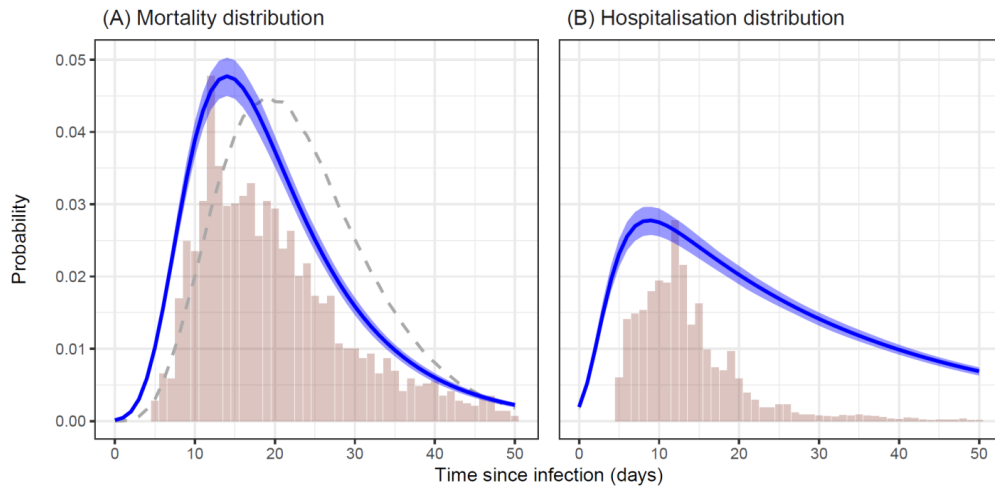
387
388 **Figure S2.** Baseline model fits to hospitalisations data for all 32 age and gender classes.
389 Shown are the model-inferred expected hospitalisation rate (lines) \pm 95% credible intervals
390 (ribbons) and the hospitalisations data used for model fitting (points).



391
392 **Figure S3.** The fit of Model 2 to daily deaths data for all 32 age and gender classes. Shown
393 are the model-inferred expected death rate from all causes (lines) \pm 95% credible intervals
394 (ribbons), and the mortality data used for model fitting (points).

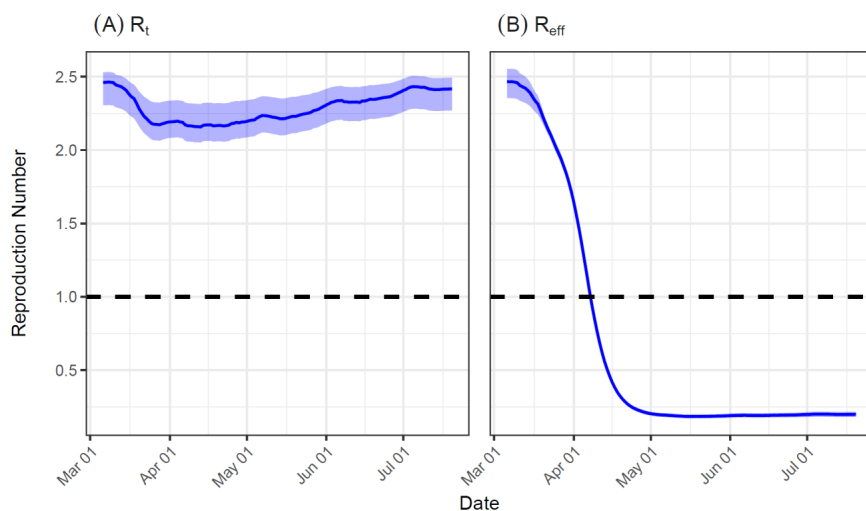


395
396 **Figure S4.** The fit of Model 2 to hospitalisations data for all 32 age and gender classes.
397 Shown are the model-inferred expected hospitalisation rate (lines) \pm 95% credible intervals
398 (ribbons) and the hospitalisations data used for model fitting (points).



399

400 **Figure S5.** Estimates from the baseline model (mean \pm 95 % credible intervals) of the shape
401 of the (A) mortality distribution and (B) hospitalisation distribution, as a function of time
402 since infection. Vertical bars indicate empirical frequencies derived from hospitalisation
403 records for Manaus. In (A), the dashed line indicates the mortality distribution used by a
404 previous COVID-19 modelling study for the State of Amazonas, Brazil¹².



405

406 **Figure S6.** Estimates from the baseline model (mean \pm 95 % credible intervals) of: (A) the
407 impact of personal mobility on the time-varying reproduction number (R_t); and (B) the
408 population-level effective reproduction number (R_{eff}) over time. In the latter, $R_{eff} < 1$ indicates
409 the switch to negative epidemic growth due to the development of herd immunity.

410 **Table S1.** Excess mortality in Manaus, Amazonas, during the COVID-19 epidemic (here
411 defined as the period between March 19 and June 24, 2020).

Age	Females			Males			Total	
	Expected mortality	Observed mortality	Excess mortality	Expected mortality	Observed mortality	Excess mortality	Total Excess mortality	Excess mortality (%)
0-5	84.5	65	-19.5	109.6	83	-26.6	-46.1	-23.7
5-10.	13.2	3	-10.2	19.3	10	-9.3	-19.5	-60
10-15.	13.5	6	-7.5	19.3	11	-8.3	-15.8	-48.2
15-20	26.1	14	-12.1	64.3	45	-19.3	-31.4	-34.7
20-25	24.1	22	-2.1	116.4	78	-38.4	-40.5	-28.8
25-30	26.7	30	3.3	92.2	81	-11.2	-7.9	-6.6
30-35	30	35	5	81.2	88	6.8	11.8	10.6
35-40	38.3	53	14.7	79	118	39	53.7	45.8
40-45	44.6	88	43.5	72.4	154	81.7	125.1	107
45-50	53.3	110	56.7	79.8	184	104.2	160.9	120.8
50-55	59.2	114	54.8	99	225	126	180.8	114.3
55-60	73.2	180	106.8	121.2	310	188.8	295.6	152.1
60-65	95.6	215	119.4	139.2	436	296.8	416.2	177.3
65-70	101.6	283	181.4	148.6	510	361.4	542.8	216.9
70-75	110.2	276	165.8	143.6	456	312.4	478.2	188.4
75+	468.4	996	527.6	382.4	1208	825.6	1353.2	159.1
Total	1262.4	2490	1227.6	1767.5	3997	2229.5	3457.2	114.1

412